

Article

# Oleo/Hydrophobic Coatings Containing Nano-Particles for the Protection of Stone Materials Having Different Porosity

Mariateresa Lettieri <sup>1,\*</sup>, Maurizio Masieri <sup>1</sup>, Alessandra Morelli <sup>2</sup>, Mariachiara Pipoli <sup>2</sup> and Mariaenrica Frigione <sup>2</sup>

<sup>1</sup> Institute of Archaeological Heritage—Monuments and Sites, CNR–IBAM, Prov.le Lecce-Monteroni, 73100 Lecce, Italy; maurizio.masieri@cnr.it

<sup>2</sup> Department of Engineering for Innovation, University of Salento, 73100 Lecce, Italy; alessmorel@tiscali.it (A.M.); mchiara.pipoli@libero.it (M.P.); mariaenrica.frigione@unisalento.it (M.F.)

\* Correspondence: mariateresa.lettieri@cnr.it; Tel.: +39-083-2422219

Received: 7 November 2018; Accepted: 23 November 2018; Published: 27 November 2018



**Abstract:** Conservation strategies to limit the degradation of stone materials are being constantly developed. To this aim, new materials are designed to confer hydrophobic properties and anti-graffiti protection to the treated surfaces. Hybrid nanocomposites, based on inorganic nano-particles added to an organic matrix, have been recently proposed for treatments of stone surfaces, obtaining promising and innovative properties. In the present paper, an experimental product based on fluorine resin containing SiO<sub>2</sub> nano-particles, a commercial fluorine-based product and a silicon-based material were applied as protective coatings on two calcareous stones (compact and porous) widely employed in the Mediterranean region. All the studied products are expected to provide both water and anti-graffiti protection to both stones' surfaces. The rheological characterization of the liquid products, changes in color of the surfaces, and variations in water vapor permeability allowed the compatibility of the protective systems applied to stones to be evaluated. Water–stone contact angle measurements and water absorption by capillarity were used to control the action against water ingress. The oleophobicity was assessed by measuring the oil–stone contact angle. The experimental nano-filled product proved to be a suitable hydrophobic coating for compact and porous stones; furthermore, it provides high oleophobicity to the treated surfaces, as required for anti-graffiti systems.

**Keywords:** stone protection; nano-particles; protective coating; hydrophobic treatments; oleophobicity

## 1. Introduction

Stone materials in buildings and monuments exposed to environmental agents undergo weathering because of many factors [1]. Water mainly contributes to the deterioration through physical, chemical and biological aging processes. Conservation strategies, designed to minimize the contact between water and stone, are adopted to avoid, or at least reduce, the weathering effects. To this aim, several types of polymers able to render hydrophobic the treated surfaces have been tested and commercialized. Acrylic, fluorinated and/or silicon-based products are typically employed as protective coatings for stone surfaces [2–11]. New materials/procedures are constantly designed to optimize products' formulation and treatment conditions [12–14]. More recently, hybrid nanocomposites based on inorganic nano-particles added to organic matrices have been proposed for the treatment of stone materials [15,16]. Promising and innovative properties have been demonstrated by these new protective products for stone and wood.

In the last few years, the application of materials providing anti-graffiti protection along with hydrophobic properties has been strongly encouraged to reduce maintenance costs and minimize

restoration interventions. For such applications, coatings exhibiting simultaneously hydrophobic and oleophobic properties must be manufactured [17–21] to prevent or limit the penetration of stain into the pores of the stone. Such materials have been successfully realized with long hydrocarbon side chains or with fluorinated components, the latter providing the oleophobic properties [22]. Other effective strategies have consisted of adding nano-particles in fluorinated polymers [23,24]. Although the importance of coatings for stone able to repel not only water but also other substances is recognized, in the current literature emphasis is placed on the protective behavior against water, while the surface oleophobicity is far less investigated.

Within this framework, a wide experimental study on three products suitable for superficial protection of stone materials has been undertaken. This research originated from a scientific collaboration running between the University of Salento and CNR-IBAM, both having well-grounded expertise in the previously mentioned topics and fields of application [25–30], in cooperation with Kimia, a well-reputed Italian company, for the production of protective coatings for stone.

An experimental formulation and two commercial products, specifically selected for comparison purposes, have been applied on two calcareous stone materials with different porosity features (compact and porous types). The commercial products are suggested for both water and anti-graffiti protection. The new nano-filled system should be suitable for the same purposes. The experimental product is based on fluorine resin containing SiO<sub>2</sub> nano-particles and has been prepared taking into account a successful formulation for hydrophobic/oleophobic coatings [24].

In this study, the rheological characterization of the liquid formulations was firstly performed to assess the suitability of the chosen application method, that is, by brush. Then, following the principle of minimum intervention, the optimal amount of product to be applied on the two stone materials was evaluated. The compatibility of the coatings with the stone materials was evaluated in terms of variation in color parameters and water vapor permeability. Then, the hydrophobic properties of the treated surfaces were investigated by water–stone static contact angle and capillary water absorption. Finally, oleophobicity was assessed by contact angle measurements using oil as wetting liquid.

## 2. Materials and Methods

### 2.1. Protective Products

An experimental formulation and, for comparison purposes, two commercial products were investigated.

The experimental product, here indicated as nanoF (Kimia S.p.A., Perugia, Italy), is a water-based fluorine resin containing 10 wt % of SiO<sub>2</sub> nano-particles 40–50 nm in dimension (data provided by Kimia S.p.A.).

In order to compare this new formulation with systems already on the market, two commercial products were selected. A first commercial product, F (Fluoline PE, C.T.S. S.r.l., Altavilla Vicentina, Vicenza, Italy), is an aqueous dispersion of fluoropolyethers (10 wt %). This material was selected because it is chemically comparable with the experimental formulation (both are fluorine-based). No information on the exact amount of product to apply is given on the technical sheet; however, it is reported that a coverage of 20 m<sup>2</sup>·L<sup>-1</sup> of product, that is, approximately 0.05 kg m<sup>-2</sup>, is guaranteed for low porous substrates. The second commercial system, SW (Kimistone DEFENDER, Kimia S.p.A., Perugia, Italy), consists of a mixture of organic silicon compounds and microcrystalline waxes in water solution. This product was chosen since belongs to a family of products, i.e., silicon-based protectives, widely used in the field of stone conservation. Quantities ranging from 0.1 to 0.3 L·m<sup>-2</sup>, depending on the porosity of the substrate, are suggested for an application on clean and dry stone surfaces.

According to the technical sheets, both F and SW are able to provide a reversible and hydrophobic coating on the treated surfaces, with dirt-repellent and anti-graffiti properties.

Details about the protective systems are listed in Table 1. Due to commercial restrictions, additional information on the chemical composition of these products is not available. The visual aspect of the three products is shown in Figure 1.

**Table 1.** Chemical composition and main details of the used products.

Product	Chemical Composition	Density (g cm <sup>-3</sup> )	pH	Visual Appearance
nanoF	Fluorine resin (12.7 wt %) and SiO <sub>2</sub> nano-particles (10 wt %) in water dispersion #	1.04 #	7–8 #	Transparent, colorless
F	Fluoropolyethers (10 wt %) in water dispersion *	1.05 *	7 *	Transparent, slightly white
SW	Mixture of organic silicon compounds and microcrystalline waxes in water solution *	0.99 *	7 *	Opaque, milky

# Data supplied by Kimia S.p.A.; \* data from the technical sheets.

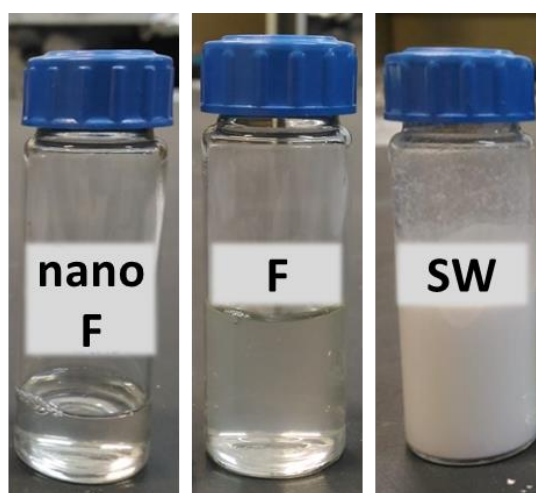


**Figure 1.** Visual aspect of the liquid products.

## 2.2. Stone Specimens

The three protective products were tested on two natural calcareous stone materials having different porosity features. A highly porous calcarenite (PS), named “Lecce stone”, and a compact limestone (CS), known as “Trani stone”, were selected. The principal constituent of “Lecce stone” is calcite (93%–97% [31]); very small quantities of clay, phosphates [32] and other non-carbonate minerals are also detected in this material [33]. Widely employed as a building material in the southeastern Italy, “Lecce stone” is typical of the Baroque architecture in this area. Due to its characteristics, “Lecce stone” can be considered as representative of porous materials used for historic and civil buildings in many countries of the Mediterranean basin, e.g., Globigerina limestone in Malta or Noto Stone in Sicily [34]. “Trani stone” is a commercial name that includes a wide array of cream-colored limestones [35] quarried in an area located north of Bari (Apulia region, Italy). Mainly composed of calcite (>95% [36]), this material also contains clay minerals and iron oxides [33]. “Trani stone” was employed in old and recent buildings, churches (such as the Cathedral of Trani) and monuments not only in southern Italy but also throughout the country [37]. One of the most famous example of its use is the mediaeval castle Castel del Monte, built by the Emperor Frederick II, inscribed on the UNESCO world heritage list since 1996.

The specimens of PS and CS used in this study exhibited an open porosity of 42% and 2%, respectively, as analyzed by mercury-intrusion porosimetry.

Prismatic stone specimens, with dimensions of 5 × 5 × 1 cm<sup>3</sup>, were cut by saw from quarry blocks. According to the UNI10921 standard protocol [38], the samples were smoothed with abrasive paper (180-grit silicon carbide), cleaned with a soft brush and washed with deionized water in order to remove dust deposits. The stone specimens were completely dried in oven at 60 °C, until the dry weight was achieved, and stored in a desiccator with silica gel (relative humidity (R.H.) = 15%) at

$23 \pm 2$  °C. Before the application of each product, the stone specimens were conditioned in equilibrium with the surrounding environment (24 h in the laboratory, at  $23 \pm 2$  °C and  $45 \pm 5\%$  R.H.).

### 2.3. Treatments

To choose the optimal quantity of nanoF product to apply on the two lithotypes, a preliminary experimental evaluation was carried out. Starting from the amount of F product proposed for the porous stone materials (i.e.,  $50 \text{ g m}^{-2}$ ), an equal quantity was applied on the CS samples. Taking into account the higher porosity of the PS samples, a triple amount (i.e.,  $150 \text{ g m}^{-2}$ ) was used on these specimens. On the other hand, also for the SW product, a triple quantity is suggested to treat porous stone materials in comparison to that employed for compact substrates. These starting amounts were applied also in duplicate and in quadruplicate on the different sample surfaces, each measuring  $25 \text{ cm}^2$ . The treatments performed in the preliminary evaluation are resumed in Table 2.

**Table 2.** Nomenclature of the treated samples and details of the treatments.

Product	PS		CS	
	Amount of Product (g/Specimen)	Coverage ( $\text{g m}^{-2}$ )	Amount of Product (g/Specimen)	Coverage ( $\text{g m}^{-2}$ )
nanoF	0.375	150	0.125	50
nanoF-2	0.750	300	0.250	100
nanoF-4	1.500	600	0.500	200

As detailed in Section 3.2, the results for optimal amounts of nanoF were  $150 \text{ g m}^{-2}$  for PS and  $50 \text{ g m}^{-2}$  for CS. Therefore, only these quantities were chosen to treat the set of samples for the complete assessment of the protective treatment. For comparison purposes, the recommended amounts of F and SW were applied on both PS and CS. The treatments were applied by brush on 3 specimens for each product to simulate the typical procedure of application in field conditions. Only one  $5 \times 5 \text{ cm}^2$  side of each specimen was treated.

The weight of the specimens was measured before and after each treatment to calculate the actual amount of product applied on the stone surfaces. After the application of the products, all the specimens were kept in the laboratory at  $23 \pm 2$  °C and  $45 \pm 5\%$  R.H. for 30 days, then they were dried in an oven at  $40$  °C until the weight stabilization was achieved; the stabilization was controlled by periodical measurements of weight.

During the preparation of the specimens, their subsequent treatments and relative tests, the environmental conditions were monitored by means of a thermo-hygrometer (Oregon Scientific, Mod. EMR812HGN), able to collect temperature data from  $-50$  to  $70$  °C (with resolution of  $0.1$  °C) and relative humidity data in the range  $2\%$ – $98\%$  (with resolution of  $\pm 1\%$ ). All weight measurements were registered using an analytical balance (Sartorius, Model BP 2215) with an accuracy of  $\pm 0.1 \text{ mg}$ .

### 2.4. Characterization Methods

#### 2.4.1. Rheological Properties of the Protective Products

A rheological analysis was performed on the liquid formulations reported in Table 1. To this aim, a strain-controlled rheometer (ARES, Rheometric Scientific, Piscataway, NJ, USA) was employed, using a plate and plate geometry (diameter of plates =  $25 \text{ mm}$ ), performing the rheological tests in steady state mode under nitrogen atmosphere. The shear rate was varied from  $0.1$  to  $100 \text{ s}^{-1}$  to assess any possible variation in viscosity as a consequence of the increase in the rate of application of the products. The test temperature was set at  $23$ – $25$  °C, i.e., representative of a typical environmental temperature in a Mediterranean region. Three experiments were performed on each formulation; the results were then averaged.

### 2.4.2. Stone Characterization

Color and contact angle measurements, water vapor transmission test and tests of water absorption by capillary were performed to characterize the untreated stone specimens.

Color measurements [39] were performed with a Konica Minolta spectrophotometer CM-700d (Konica Minolta Sensing, Singapore), using CIE Standard illuminant D65 and the target mask 8 mm in diameter. Ten measurements were performed on each specimen and the instrument was recalibrated to a white calibration cap at the start of each measurement session. The color coordinates were expressed in the CIE  $L^* a^* b^*$  color space (1976), where:  $L^*$  is the lightness/darkness coordinate, ranging from 0 (black) to 100 (white);  $a^*$  is the red/green coordinate, with positive values related to red while negative ones to green;  $b^*$  is the yellow/blue coordinate, with positive values related to yellow and negative to blue.

Water–stone static contact angle measurements were carried out on 30 different positions of the surface for each specimen, according to the European standard [40]. A Costech apparatus was used to deposit micro-drops of deionized water on the stone surfaces. The shape of the drop was recorded with a camera and the related contact angle was calculated by means of the “anglometer 2.0” software (Costech). To assure the reproducibility of the test, the image of each drop was acquired 15 s after its deposition. For the untreated PS material, the water absorption was very high and rapid; as a consequence, the drops of water were suddenly absorbed inside the porous stone and the contact angle was not determinable.

The water vapor transport properties of untreated stone materials were evaluated at 20 °C by the vapor transmission test described in [26]. Throughout the experiment, the containers with the samples were placed into desiccators with silica gel and stored in a climatic chamber (Mod. UY 600, ACS Angelantoni Climatic Systems, Massa Martana, Perugia, Italy) at 20 °C. Weight measurements were carried out every 24 h in order to determine the rate of vapor transport through the sample from the water (in the container, the R.H. was very close to 100%) to the controlled atmosphere of the desiccator (R.H. 15%, 1 atm). The cumulative mass decrease was plotted versus time and the water vapor flow rate ( $G$ ) was calculated as the slope of the curve.

The water vapor transmission rate (WVTR) was evaluated as the mass of water vapor passing through the surface unit in the unit time (24 h). This parameter is referred to as permeability in [41]. The following equation was used:

$$\text{WVTR} = \Delta M / (t \cdot A) \quad (1)$$

where:  $\Delta M$  is the weight change in the steady state (g);  $A$  is the area exposed to water vapor ( $\text{m}^2$ ); and  $t$  is the unit time (24 h). In our case,  $\Delta M$  was calculated as the average of five consequent values of the daily difference in weight and the exposed area was  $0.001611 \text{ m}^2$ .

The capillarity water absorption test was performed according to the procedure described in the European standard [42]. The amount of absorbed water ( $Q$ ) was calculated as follows:

$$Q_i = (w_i - w_0) / A \quad (2)$$

where:  $w_i$  and  $w_0$  are the weight of the sample at time  $t_i$  and  $t_0$ , respectively;  $A$  is the area exposed to water.  $Q_i$  values were plotted versus the square root of time to evaluate the water absorption.

### 2.4.3. Preliminary Evaluation of the Optimal Amount of Product for Each Treatment

In order to achieve the maximum preservation of the stone materials with the minimum intervention, the amount of each product yielding the lowest color variation along with the highest contact angle was identified. A similar screening was successful applied for treatments on Lecce stone in a previous study [43].

After the application of the product, as described in Section 2.3, color and water–stone static contact angle measurements were performed on the treated stone surfaces. These investigations were

carried out on the same specimens previously examined without any protective treatment and the changes in color and in surface wettability were evaluated as differences in the same untreated areas.

The difference in color ( $\Delta E^*_{ab}$ ) before and after the coating application was calculated through the following formula:

$$\Delta E^*_{ab} = [(L^*_u - L^*_t)^2 + (a^*_u - a^*_t)^2 + (b^*_u - b^*_t)^2]^{1/2} \quad (3)$$

where: the subscript “u” refers to the uncoated surfaces; the subscript “t” refers to the treated samples.

#### 2.4.4. Assessment of Coatings' Compatibility with the Substrates and Hydrophobic Properties

After the application of each protective treatment, color parameters, water–stone static contact angle, water vapor permeability and capillary water absorption were measured on the coated samples. The same procedures employed for the untreated specimens were adopted.

In addition, the reduction of the vapor permeability (RVP) was quantified as follows [26,44]:

$$\text{RVP}\% = [(\Delta M_u - \Delta M_t) / \Delta M_u] \times 100 \quad (4)$$

where:  $\Delta M_u$  is the weight change in the steady state for the untreated sample;  $\Delta M_t$  is the same parameter calculated for the coated sample. The  $\Delta M$  used in the previous equation was the average of five consequent values of the daily difference in weight.

Aesthetic properties and water vapor permeability were used to assess the compatibility of each coating with the stone materials; contact angle and water absorption measurements allowed evaluating the hydrophobic properties in the presence of the different coatings.

#### 2.4.5. Evaluation of the Oleophobicity

Following a procedure already proposed in other studies [21,24], static contact angles were determined using commercial olive oil (purchased from a local market) in order to test the coating oleophobicity. The used apparatus and procedure were the same described in Section 2.4.2.

As in the measurements of water contact angles, the image of each drop was acquired 15 s after the deposition. In the untreated PS material, the drop of oil was slowly absorbed but disappeared within 15 s. Consequently, the oil contact angle was not determinable on these surfaces. Since the oil drops irretrievably stained the untreated specimens, these samples were not used for the treatments. Therefore, this test was not performed on the same areas before and after the application of the coatings.

The reported oil–stone contact angles are the averages of five measurements, carried out on different spots of each sample.

### 3. Results and Discussion

#### 3.1. Rheological Properties of the Liquid Products

The measurement of the viscosity of a protective coating in liquid state (i.e., before its application) is particularly important from an applicative point of view. This parameter, in fact, allows assessing if the conventional techniques typically employed to apply the product on the substrate (in this case by brush) are suitable. In addition, the viscosity of the organic matrix should not be appreciably impaired by the presence of nano-particles.

In Figure 2, the viscosity of the three liquid products under analysis, i.e., nanoF, F and SW, is reported as a function of the shear rate. It can be observed that all the liquid products display a pseudo-plastic behavior, being the viscosity of the experimental product, nanoF, comparable or slightly greater than those measured on both the commercial products, i.e., F and SW, at least in the shear rate range analyzed. The obtained results confirm that the new nano-filled product exhibits a viscosity still appropriate for the proposed purpose, as previously reported for different nano-filled protective products [45]. The experimental formulation can be applied, therefore, by brush on stone substrates

and its viscosity allows an appropriate penetration into the porous structure of the stone substrates, assuring a good grip on the surface requiring protection.

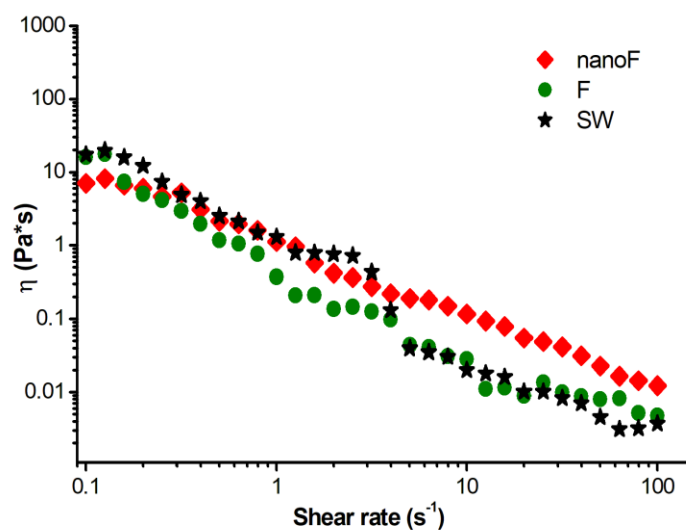


Figure 2. Viscosity of the liquid formulations as a function of the shear rate.

### 3.2. Determination of the Appropriate Amount of nanoF Product

Color differences and water–stone static contact angle values, determined on the untreated stone samples as well as after their treatments with nanoF product (as detailed in Section 2.3), are reported in Table 3.

Table 3. Color difference ( $\Delta E^*_{ab}$ ) and water–stone static contact angle (WCA), with the relative standard deviations, before (b.t.) and after (a.t.) the treatments with nanoF product.

Stone Support	Samples	Actual Applied Amount ( $\text{g m}^{-2}$ )	$\Delta E^*_{ab}$ (CIELAB Unit)	WCA ( $^\circ$ )	
				b.t.	a.t.
PS	nanoF	153	1.13	n.d.	145 ± 3
	nanoF-2	305	2.03	n.d.	146 ± 2
	nanoF-4	611	2.58	n.d.	146 ± 2
CS	nanoF	56	1.02	31 ± 4	141 ± 6
	nanoF-2	105	1.00	42 ± 7	142 ± 4
	nanoF-4	205	2.99	29 ± 8	145 ± 4

n.d. = not determinable.

In the case of PS samples, color changes increased as the applied quantity of nanoF increased, still remaining satisfactory. In fact, all the color variations measured on PS were lower than the values perceivable by a human eye (i.e.,  $\Delta E^*_{ab} = 3$  [46–48]).

As already explained above, the water–stone contact angle cannot be determined on untreated PS stone. Very high contact angle values ( $\geq 145^\circ$ ) were recorded on all the samples treated with nanoF product, irrespective of the applied amounts. In addition, an interesting phenomenon was observed for nanoF-2 and nanoF-4 samples. In the latter cases, more than 50% of the measurement points exhibited complete repellence of the micro-drops of water (Figure 3).

Low color variations were measured on CS specimens after the application of the smallest amount of nanoF. Similar color changes were obtained using a doubled quantity of protective product;  $\Delta E^*_{ab}$  values close to those visible by the naked eye were found further increasing the applied amount of nanoF.

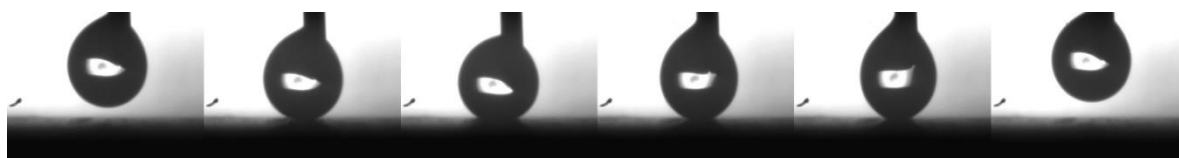


**Figure 3.** Contact angle measurement on the PS-nanoF-2 sample: from left to right, the pendant water drop touches the stone sample, the droplet does not stick onto the treated surface but remains attached to the needle.

Contact angles higher than  $140^\circ$  were measured on all the CS surfaces treated with nanoF product; no clear dependence on the applied amount was observed. Unlike the PS samples, total repellence of water drops was never observed.

According to the minimum intervention criteria, the lowest amounts of nanoF (i.e., 150 and  $50 \text{ g m}^{-2}$  for PS and CS, respectively) used in these preliminary tests were selected to complete the evaluation of the protective treatment. These quantities, in fact, proved suitable to obtain highly hydrophobic surfaces along with minimal color changes. Due to the high open porosity, a greater amount of product was necessary to achieve good performances in the porous stone.

### 3.3. Compatibility of the Coatings with the Stone Materials

#### 3.3.1. Aesthetic Aspect

The variation in color parameters and the actual amount of each product applied on the stone substrates are listed in Table 4. The related total color variations (expressed as  $\Delta E^*_{ab}$ ) are reported in Figure 4.

**Table 4.** Amount of applied product, color changes as variations of  $L^*$ ,  $a^*$ , and  $b^*$  measured before and after the coating application. The standard deviation is reported for each data set.

Stone Support	Treatment	Actual Applied Amount ( $\text{g m}^{-2}$ )	$\Delta L^*$	$\Delta a^*$	$\Delta b^*$
PS	nanoF	$155 \pm 3$	$-0.13 \pm 0.10$	$-0.12 \pm 0.12$	$1.38 \pm 0.12$
	F	$160 \pm 5$	$-1.50 \pm 0.22$	$0.03 \pm 0.07$	$3.66 \pm 0.36$
	SW	$313 \pm 2$	$-1.92 \pm 0.22$	$0.14 \pm 0.13$	$2.94 \pm 0.12$
CS	nanoF	$58 \pm 6$	$-0.98 \pm 0.40$	$0.08 \pm 0.08$	$1.72 \pm 0.39$
	F	$60 \pm 5$	$-1.48 \pm 0.32$	$0.21 \pm 0.07$	$2.50 \pm 0.42$
	SW	$109 \pm 7$	$-1.82 \pm 0.52$	$0.28 \pm 0.07$	$1.78 \pm 0.24$

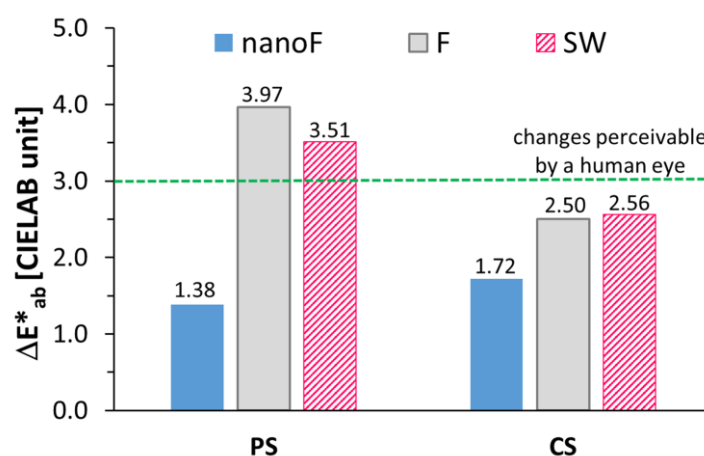


**Figure 4.** Differences in color ( $\Delta E^*_{ab}$ ) before and after the products' application.

The treatment of both stone substrates with nanoF product did not produce significant color changes. Very low variations for  $L^*$  and  $a^*$  and a small increase in  $b^*$  were, in fact, recorded. A slightly higher  $\Delta E^*_{ab}$  was measured for CS samples, although a lower quantity of product was applied.

Larger color variations were measured on PS samples treated with F product, even with amounts of product comparable to those used for the nanoF treatment. The SW product, applied in a double quantity, yielded similar results. In both these cases, the measured  $\Delta E^*_{ab}$  were higher than 3, the value referred as perceivable by a human eye, but still below the threshold ( $\Delta E^*_{ab} \leq 5$ ) judged tolerable in conservation interventions of built heritage [46,49,50]. Actually, a weak yellowing of the treated PS surfaces was observed (Figure 5), also supported by the increase in the  $b^*$  parameter (Table 4).



Figure 5. Uncoated and coated PS stone surfaces.

The treatments with F and SW on the CS samples produced higher color changes in comparison to surfaces treated with nanoF formulation. However, these changes were not clearly visible to the naked eye (Figure 6) and the  $\Delta E^*_{ab}$  remained below 3 (Figure 4).

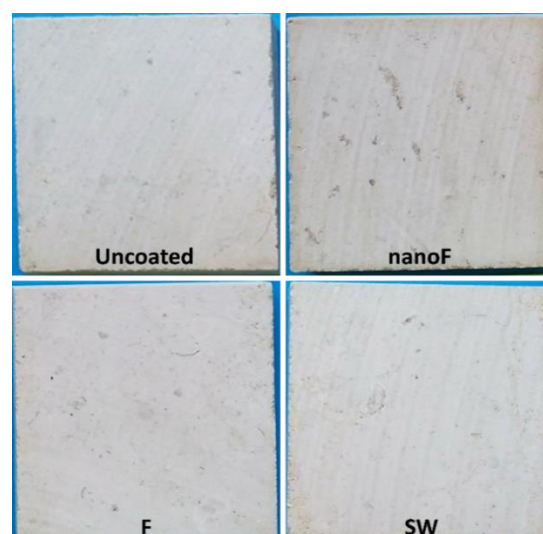
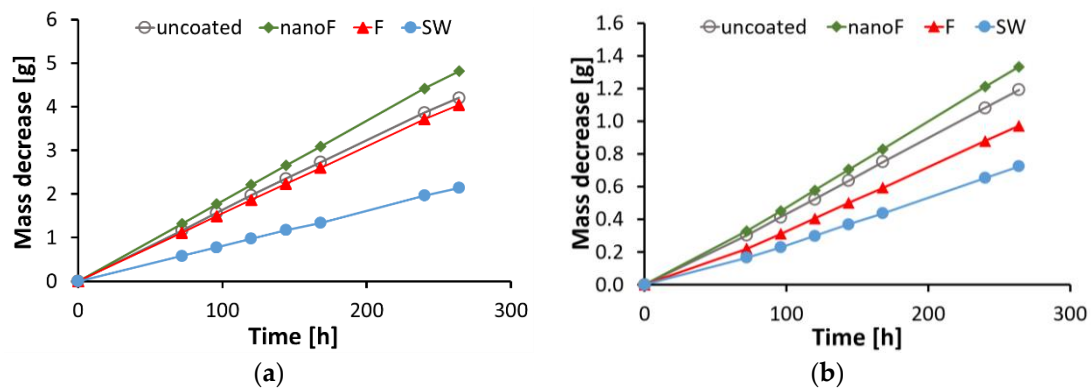


Figure 6. Uncoated and coated CS stone surfaces.

### 3.3.2. Water Vapor Transport Properties

Along with the absence of appreciable color variations, changes in the water vapor transport properties of coated stone materials should be avoided. Reduction in permeability may cause water condensation inside the stone, which accumulation at the interface between the treated and untreated stone regions may activate the material's decay [26].

In Figure 7, the mass changes measured during the vapor transmission test are plotted for all the treatments and the two stone substrates. For all the samples, linear trends were observed and the steady state was noticed 96 h after the beginning of the test.



**Figure 7.** Variations of mass measured during the vapor transmission test for uncoated and coated (a) PS and (b) CS stone surfaces.

The greatest reductions of the water vapor transport parameters were obtained for the stone specimens coated with SW product, confirmed by data reported in Table 5. A more pronounced decrease was measured in the PS samples, where the highest amount of SW was applied. Although these results are close to those reported in the literature for many siloxane-based coatings applied to stone materials [51–53], the permeability decrease, i.e., RVP, exceeded the acceptable threshold of 20% [54].

**Table 5.** Water vapor flow rate (G), water vapor transmission rate (WVTR), both before (b.t.) and after (a.t.) the treatment, and reduction of vapor permeability (RVP). Standard deviations are reported for each data set.

Stone Support	Samples	$G [(g\ h^{-1}) \cdot 10^{-3}]$		WVTR [ $g\ m^{-2} \cdot 24\ h$ ]		RVP [%]
		b.t.	a.t.	b.t.	a.t.	
PS	nanoF	$16.1 \pm 1.4$	$18.4 \pm 5.6$	$189 \pm 17$	$216 \pm 66$	−14
	F	$16.4 \pm 0.8$	$15.4 \pm 2.3$	$191 \pm 11$	$180 \pm 24$	6
	SW	$17.0 \pm 0.9$	$8.1 \pm 2.1$	$199 \pm 10$	$97 \pm 27$	51
CS	nanoF	$4.4 \pm 0.2$	$5.1 \pm 1.4$	$53 \pm 2$	$61 \pm 16$	−15
	F	$4.0 \pm 0.6$	$3.7 \pm 0.1$	$48 \pm 6$	$45 \pm 2$	5
	SW	$4.5 \pm 0.2$	$2.7 \pm 0.3$	$54 \pm 2$	$34 \pm 3$	38

A better performance was obtained by treating both stone supports with the fluoropolyethers-based formulation, i.e., F product. Here, just slight decreases in the water vapor transport parameters measured for the untreated stone samples were noticed.

Conversely, increases in permeability were obtained after the application of the nanoF product, irrespective to the porosity of the stone. Other researchers have highlighted the same phenomenon in stone samples [55,56] and in membranes [57] treated or functionalized with highly hydrophobic thin coatings. An improvement of water vapor transport was noticed also when nano-particles have been added to a protective coating [52]. In these studies, a lower condensation of water molecules on the

hydrophobic pore walls was hypothesized in the treated samples. As a consequence, the diffusion of water vapor through hydrophobic pores was enhanced and permeability increased. This effect was not observed where the polymer layer onto the pore walls was thick enough to reduce the pore dimensions.

### 3.4. Hydrophobic Properties

#### 3.4.1. Surface Wettability

The results of water–stone static contact angle measurements, reported in Table 6, show that all the applied coatings lead to a significant reduction in the surface wettability. The character of the stone surfaces, in fact, changed from hydrophilic, before the treatment, to hydrophobic after the application of each coating, as witnessed by an appreciable increase in contact angle values. This effect was particularly evident in the case of PS substrate, for which the starting condition was the immediate and complete absorption of the water drop. After the treatments, the measured contact angles ranged between 119° and 142° for PS samples, and between 106° and 139° for CS surfaces. In agreement with other studies [58,59], the presence of the SiO<sub>2</sub> nano-particles further increased the hydrophobicity of the surface brought about by the application of a fluoropolyethers-based coating. The highest contact angles were, in fact, measured on the coating containing the nano-particles, with values of approximately 140°, irrespective of the stone substrate. The low standard deviation values found for all the treated samples accounted for a homogeneous distribution of the products on the sample surface.

**Table 6.** Water–stone static contact angle (°) measured on each stone, along with the standard deviation, before (b.t.) and after (a.t.) each treatment.

Samples	PS		CS	
	b.t.	a.t.	b.t.	a.t.
nanoF	Not determinable	142 ± 5	39 ± 8	139 ± 5
F	Not determinable	119 ± 3	46 ± 8	106 ± 4
SW	Not determinable	122 ± 4	36 ± 9	114 ± 4

#### 3.4.2. Capillary Water Absorption

The curves of water absorption by capillarity for the samples before and after each treatment are reported in Figure 8. As expected, different behaviors in water absorption were observed because of the different porosity features. However, it can be generally noticed that the water absorption was reduced by the presence of a coating in the early steps of the test, but the protective action was lost at longer contact times. Only the PS samples treated with the SW product exhibited a good behavior in terms of long-term water repellence. This result was explained in terms of the greater amount of this product applied on PS surfaces.

Generally speaking, a very low water absorption by capillarity is expected if a low wettability is obtained by the application of a water-repellent coating. In this case, the water uptake after the treatments was only partially, and for a limited contact time, reduced, in disagreement with the high contact angle values measured on the same coated specimens. Similar results were found by other researchers, especially using nano-filled polymeric coatings [60,61], and they were ascribed to different penetration of the products and interaction with the substrate [62]. It is to point out that these two tests, i.e., contact angle measurements and capillary water absorption tests, are complementary and cannot provide the same information. The capillary absorption test evaluates the long-term water uptake, over the entire area of the specimen; the contact angle, on the other hand, measures the hydrophobicity at the interface between the droplet and the stone surface, at a very short contact time.

It must be underlined, in conclusion, that the capillary water absorption behavior of the experimental nanoF product applied to both stone surfaces is in some way comparable to the performance of commercial protective products.

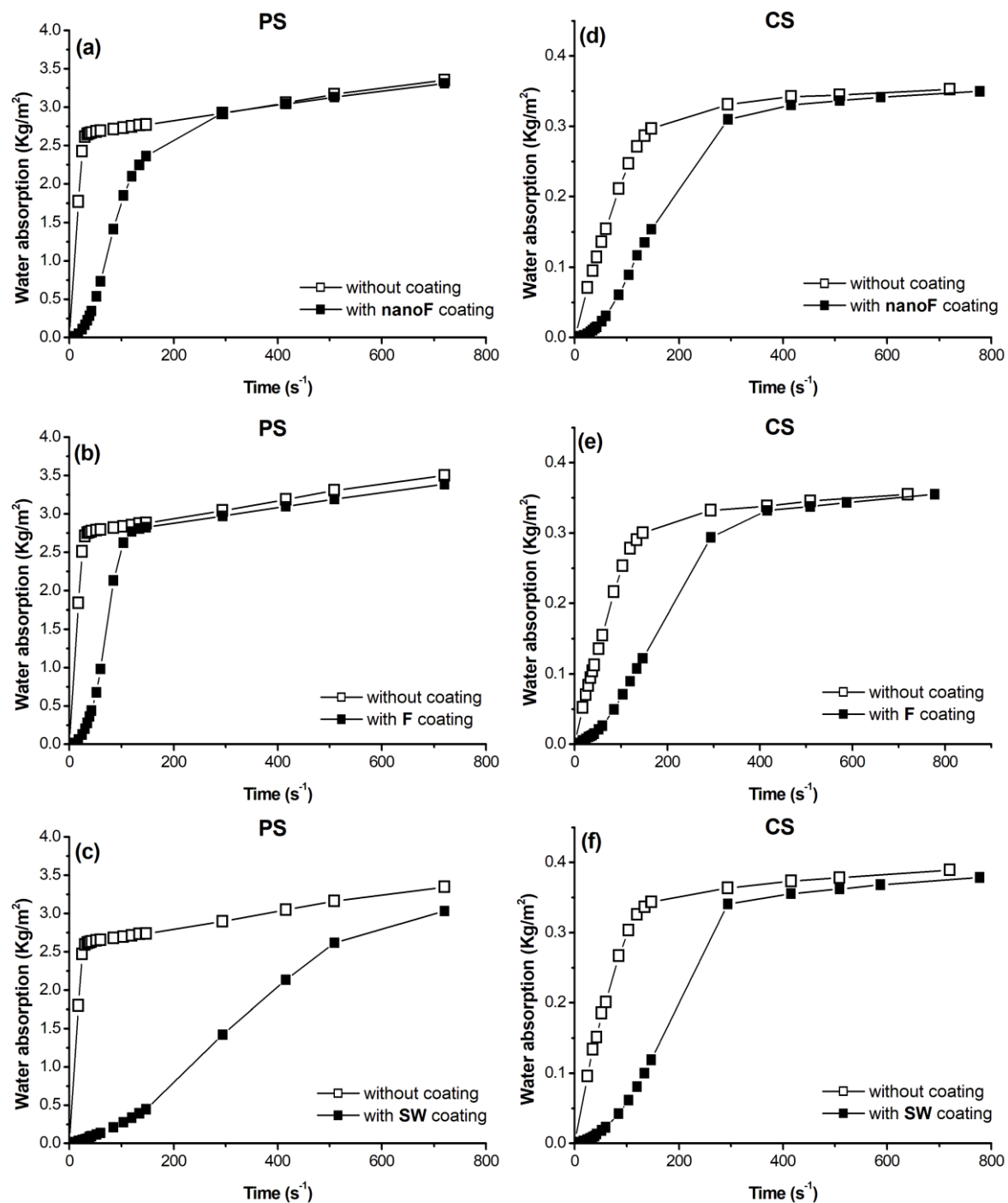


**Figure 8.** Capillary water absorption curves: (a–c) PS specimens with and without the nanoF, F and SW coatings, respectively; (d–f) CS specimens with and without the nanoF, F and SW coatings, respectively.

### 3.5. Oleophobicity

The measurement of the static oil contact angle is a common simple method to assess the oil-repellence of a surface. Values greater than 70–80 degrees account for oleophobic surfaces [23,63].

Due to the low surface tension of the oil drops in comparison to that of the water ( $72 \text{ mN m}^{-1}$  for water [21],  $32 \text{ mN m}^{-1}$  for olive oil [64]), lower oil contact angles were measured, summarized in Table 7. The highest values were measured when nanoF coating was applied, irrespective to the kind of stone. The surfaces treated with the fluorinated product F were also oleophobic, being the oil contact angles above  $90^\circ$ . On the other hand, values of  $56^\circ$  were determined for the SW coating,

on both PS and CS specimens. In this latter case, no fluorinated groups, generally able to provide oil-repellence in coatings [65], are present in the SW product.

**Table 7.** Oil–stone static contact angle ( $^{\circ}$ ) measured on untreated and treated PS and CS stone surfaces, with the indication of standard deviation.

Samples	PS	CS
Untreated	Not determinable	13 $\pm$ 1
nanoF	122 $\pm$ 7	114 $\pm$ 1
F	114 $\pm$ 4	93 $\pm$ 4
SW	56 $\pm$ 2	56 $\pm$ 1

The result obtained from the oil–stone contact angle measurements allowed the new nanoF product to be considered suitable for anti-graffiti applications. Further studies are in progress to confirm the anti-stain feature supplied to stone materials by the experimental nano-filled coating.

#### 4. Conclusions

In this study, an experimental formulation, based on fluorine resins and SiO<sub>2</sub> nano-particles, was tested on two calcareous stone materials, with different porosity, widely employed in the Mediterranean region. The harmlessness of the treatments and their efficacy for protection against water ingress, as well as their potential anti-graffiti applications, were evaluated. A comparison with two commercial protective products was also done.

The rheological tests showed that the viscosity of the new nanoF product is suitable for application by brush and allows an appropriate penetration into the stone substrates. To achieve good and comparable performances, a triple dose of product was necessary for the treatment of the porous stone. Low color changes, below the  $\Delta E^*_{ab}$  value of 3, referred as perceivable by a human eye, were measured after the application of the nanoF product on the stone surfaces. Conversely, the two commercial products caused more marked variations, in particular in the porous stone. These variations, in some cases, were visible to the naked eye, but still lower than the threshold judged tolerable in conservation interventions of built heritage. Water vapor transport properties declined in the samples treated with the commercial coating products. Unacceptable permeability reductions were calculated in the cases of specimens coated with SW product; negligible decreases were observed when F formulation was applied. Unexpected improvement in permeability was measured after the application of the experimental nanoF product, probably due to the high hydrophobicity of the pore walls inside the stone brought about by the application of the nano-filled coating. The water absorption by capillarity was not adequately limited, irrespective of the product applied, although all the coated surfaces exhibited a low wettability. The water–stone contact angles ranged between 106 $^{\circ}$  and 142 $^{\circ}$ , with the highest values measured for the nanoF coatings. Additional investigations are in progress to try to understand the wetting behavior observed in these coated surfaces. Additionally, the nanoF coating gave rise to good results in terms of oleophobicity. No significant differences were found using different stone substrates. In fact, the results were comparable for both the compact and porous stone.

It is important to highlight that the efficacy of the nanoF treatment, comparable or even better than those displayed by commercial systems, was obtained through applying smaller amounts of product to the stone.

In conclusion, this experimental product can be suggested as protective coating for stone against water ingress, but also for anti-graffiti applications. The evaluation of the resistance to staining agents, along with the related cleaning/removal procedures, are currently being investigated and will be the subject of a forthcoming paper. Since no significant differences were found using different stone substrates, the new product can be proposed for both compact and porous stone materials. Finally, the achievement of satisfactory properties through the application of low quantities of product allows the

balancing of the requirements of the conservative actions and their sustainability, in particular in terms of costs and environmental impact.

**Author Contributions:** Conceptualization, M.L. and M.F.; Formal Analysis, M.L., M.M. and M.F.; Investigation, M.M., A.M. and M.P.; Writing-Review & Editing, M.L. and M.F.; Supervision, M.F.

**Funding:** This research received no external funding.

**Acknowledgments:** The work is the outcome of a scientific collaboration carried out with Kimia Company (Perugia, Italy), which supplied the experimental (nanoF) product under investigation. To this regards, the Authors wish to thank Assorestauro Association, and the Advisor of the Board Arch. Cristina Caiulo, for the scientific networking created between University of Salento and Kimia Company.

**Conflicts of Interest:** The authors declare no conflicts of interest.

## References

1. Steiger, M.; Charola, A.E.; Sterflinger, K. Weathering and Deterioration. In *Stone in Architecture: Properties, Durability*; Siegesmund, S., Snethlage, R., Eds.; Springer: Berlin, Germany, 2014; pp. 225–316.
2. Horie, C.V. *Materials for Conservation: Organic Consolidants, Adhesives and Coatings*; Routledge: London, UK, 2010.
3. Toniolo, L.; Poli, T.; Castelvetro, V.; Manariti, A.; Chiantore, O.; Lazzari, M. Tailoring new fluorinated acrylic copolymers as protective coatings for marble. *J. Cult. Herit.* **2002**, *3*, 309–316. [[CrossRef](#)]
4. Vicini, S.; Mariani, A.; Princi, E.; Bidali, S.; Pincin, S.; Fiori, S.; Pedemonte, E.; Brunetti, A. Frontal polymerization of acrylic monomers for the consolidation of stone. *Polym. Adv. Technol.* **2005**, *16*, 293–298. [[CrossRef](#)]
5. Tsakalof, A.; Manoudis, P.; Karapanagiotis, I.; Chrysoulakis, I.; Panayiotou, C. Assessment of synthetic polymeric coatings for the protection and preservation of stone monuments. *J. Cult. Herit.* **2007**, *8*, 69–72. [[CrossRef](#)]
6. Vacchiano, C.D.; Incarnato, L.; Scarfato, P.; Acierno, D. Conservation of tuff-stone with polymeric resins. *Constr. Build. Mater.* **2008**, *22*, 855–865. [[CrossRef](#)]
7. Torrisi, A. Evaluation of five fluorinated compounds as calcarenite protectives. *J. Cult. Herit.* **2008**, *9*, 135–145. [[CrossRef](#)]
8. Esposito Corcione, C.; Frigione, M. UV-cured siloxane-modified acrylic coatings containing birifrangent calcarenitic stone particles: Photo-calorimetric analysis and surface properties. *Prog. Org. Coat.* **2011**, *72*, 522–527. [[CrossRef](#)]
9. Licchelli, M.; Malagodi, M.; Weththimuni, M.L.; Zanchi, C. Water-repellent properties of fluoroelastomers on a very porous stone: Effect of the application procedure. *Prog. Org. Coat.* **2013**, *76*, 495–503. [[CrossRef](#)]
10. Ugur, I. Surface characterization of some porous natural stones modified with a waterborne fluorinated polysiloxane agent under physical weathering conditions. *J. Coat. Technol. Res.* **2014**, *11*, 639–649. [[CrossRef](#)]
11. Fermo, P.; Cappelletti, G.; Cozzi, N.; Padeletti, G.; Kaciulis, S.; Brucale, M.; Merlini, M. Hydrophobizing coatings for cultural heritage. A detailed study of resin/stone surface interaction. *Appl. Phys. A* **2014**, *116*, 341–348. [[CrossRef](#)]
12. Sabatini, V.; Cattò, C.; Cappelletti, G.; Cappitelli, F.; Antenucci, S.; Farina, H.; Ortenzi, M.A.; Camazzola, S.; Di Silvestro, G. Protective features, durability and biodegradation study of acrylic and methacrylic fluorinated polymer coatings for marble protection. *Prog. Org. Coat.* **2018**, *114*, 47–57. [[CrossRef](#)]
13. Camaiti, M.; Brizi, L.; Bortolotti, V.; Papacchini, A.; Salvini, A.; Fantazzini, P. An Environmental Friendly Fluorinated Oligoamide for Producing Nonwetting Coatings with High Performance on Porous Surfaces. *ACS Appl. Mater. Interfaces* **2017**, *9*, 37279–37288. [[CrossRef](#)] [[PubMed](#)]
14. Cao, Y.; Salvini, A.; Camaiti, M. Oligoamide grafted with perfluoropolyether blocks: A potential protective coating for stone materials. *Prog. Org. Coat.* **2017**, *111*, 164–174. [[CrossRef](#)]
15. Frigione, M.; Lettieri, M. Novel Attribute of Organic-Inorganic Hybrid Coatings for Protection and Preservation of Materials (Stone and Wood) Belonging to Cultural Heritage. *Coatings* **2018**, *8*. [[CrossRef](#)]
16. Hosseini, M.; Karapanagiotis, I. *Advances Materials for Conservation of Stone*; Springer: Cham, Switzerland, 2018.

17. Malaga, K.; Mueller, U. Relevance of Hydrophobic and Oleophobic Properties of Antigrffiti Systems on Their Cleaning Efficiency on Concrete and Stone Surfaces. *J. Mater. Civ. Eng.* **2013**, *25*, 755–762. [[CrossRef](#)]
18. Kronlund, D.; Lindén, M.; Smått, J.-H. A sprayable protective coating for marble with water-repellent and anti-graffiti properties. *Prog. Org. Coat.* **2016**, *101*, 359–366. [[CrossRef](#)]
19. Godeau, G.; Guittard, F.; Darmanin, T. Surfaces Bearing Fluorinated Nucleoperfluorolipids for Potential Anti-Graffiti Surface Properties. *Coatings* **2017**, *7*, 220. [[CrossRef](#)]
20. Zarzuela, R.; Luna, M.; Carrascosa, L.A.M.; Mosquera, M.J. Preserving Cultural Heritage Stone: Innovative Consolidant, Superhydrophobic, Self-Cleaning, and Biocidal Products. In *Advanced Materials for the Conservation of Stone*; Hosseini, M., Karapanagiotis, I., Eds.; Springer: Cham, Switzerland, 2018; pp. 259–275.
21. Aslanidou, D.; Karapanagiotis, I.; Panayiotou, C. Tuning the wetting properties of siloxane-nanoparticle coatings to induce superhydrophobicity and superoleophobicity for stone protection. *Mater. Des.* **2016**, *108*, 736–744. [[CrossRef](#)]
22. Sepeur, S.; Frenzer, G. Commercial Applications of Nanocomposite Sol-Gel Coatings. In *Sol-Gel Nanocomposites*; Guglielmi, M., Kickelbick, G., Martucci, A., Eds.; Springer: New York, NY, USA, 2014; pp. 191–221.
23. Basu, B.J.; Bharathidasan, T.; Anandan, C. Superhydrophobic oleophobic PDMS-silica nanocomposite coating. *Surf. Innov.* **2013**, *1*, 40–51. [[CrossRef](#)]
24. Facio, D.S.; Carrascosa, L.A.M.; Mosquera, M.J. Producing lasting amphiphobic building surfaces with self-cleaning properties. *Nanotechnology* **2017**, *28*, 265601. [[CrossRef](#)] [[PubMed](#)]
25. Calia, A.; Colangiuli, D.; Lettieri, M.; Matera, L. A deep knowledge of the behaviour of multi-component products for stone protection by an integrated analysis approach. *Prog. Org. Coat.* **2013**, *76*, 893–899. [[CrossRef](#)]
26. Lettieri, M.; Masieri, M. Performances and Coating Morphology of a Siloxane-Based Hydrophobic Product Applied in Different Concentrations on a Highly Porous Stone. *Coatings* **2016**, *6*, 60. [[CrossRef](#)]
27. Esposito Corcione, C.; Striani, R.; Frigione, M. Organic-inorganic UV-cured methacrylic-based hybrids as protective coatings for different substrates. *Prog. Org. Coat.* **2014**, *77*, 1117–1125. [[CrossRef](#)]
28. Esposito Corcione, C.; Manno, R.; Frigione, M. Sunlight curable boehmite/siloxane-modified methacrylic nano-composites: An innovative solution for the protection of carbonate stones. *Prog. Org. Coat.* **2016**, *97*, 222–232. [[CrossRef](#)]
29. Esposito Corcione, C.; De Simone, N.; Santarelli, M.L.; Frigione, M. Protective properties and durability characteristics of experimental and commercial organic coatings for the preservation of porous stone. *Prog. Org. Coat.* **2017**, *103*, 193–203. [[CrossRef](#)]
30. Masieri, M.; Lettieri, M. Influence of the Distribution of a Spray Paint on the Efficacy of Anti-Graffiti Coatings on a Highly Porous Natural Stone Material. *Coatings* **2017**, *7*, 18. [[CrossRef](#)]
31. Bugani, S.; Camaiti, M.; Morselli, L.; Van de Castele, E.; Janssens, K. Investigation on porosity changes of Lecce stone due to conservation treatments by means of X-ray nano- and improved micro-computed tomography: Preliminary results. *X-Ray Spectrom.* **2007**, *36*, 316–320. [[CrossRef](#)]
32. Föllmi, K.B.; Hofmann, H.; Chiaradia, M.; de Kaenel, E.; Frijia, G.; Parente, M. Miocene phosphate-rich sediments in Salento (southern Italy). *Sediment. Geol.* **2015**, *327*, 55–71. [[CrossRef](#)]
33. Tiano, P.; Accolla, P.; Tomaselli, L. Phototrophic biodeteriogens on lithoid surfaces: An ecological study. *Microb. Ecol.* **1995**, *29*, 299–309. [[CrossRef](#)] [[PubMed](#)]
34. Franzoni, E.; Sassoni, E.; Graziani, G. Brushing, poultice or immersion? The role of the application technique on the performance of a novel hydroxyapatite-based consolidating treatment for limestone. *J. Cult. Herit.* **2015**, *16*, 173–184. [[CrossRef](#)]
35. Borghi, A.; Berra, V.; D’atri, A.; Dino, G.A.; Gallo, L.M.; Giacobino, E.; Martire, L.; Massaro, G.; Vaggelli, G.; Bertok, C.; et al. Stone materials used for monumental buildings in the historical centre of Turin (NW Italy): Architectonical survey and petrographic characterization of Via Roma. *Geol. Soc. Lond. Spec. Publ.* **2014**, *407*, 201–218. [[CrossRef](#)]
36. Sassoni, E.; Franzoni, E. Influence of porosity on artificial deterioration of marble and limestone by heating. *Appl. Phys. A* **2014**, *115*, 809–816. [[CrossRef](#)]
37. Gambino, F.; Borghi, A.; d’Atri, A.; Gallo, L.M.; Ghiraldi, L.; Giardino, M.; Martire, L.; Palomba, M.; Perotti, L.; Macadam, J. TOURinSTONES: A Free Mobile Application for Promoting Geological Heritage in the City of Torino (NW Italy). *Geoheritage* **2017**, 1–15. [[CrossRef](#)]

38. UNI 10921 Beni Culturali Materiali Lapidei Naturali ed Artificiali–Prodotti Idrorepellenti–Applicazione su Provini e Determinazione in Laboratorio Delle Loro Caratteristiche; Ente Italiano di normazione: Milan, Italy, 2001.
39. EN 15886 Conservation of Cultural Property–Test Methods–Colour Measurement of Surfaces; CEN (European Committee for Standardization): Brussels, Belgium, 2010.
40. EN 15802 Conservation of Cultural Property–Test Methods–Determination of Static Contact Angle; CEN (European Committee for Standardization): Brussels, Belgium, 2010.
41. NORMAL Rec. 21/85 Permeabilità al Vapor D’acqua; C.N.R.: Rome, Italy, 1985. (In Italian)
42. EN 15801 Conservation of Cultural Property–Test Methods–Determination of Water Absorption by Capillarity; CEN (European Committee for Standardization): Brussels, Belgium, 2009.
43. Calia, A.; Lettieri, M.; Matera, L.; Sileo, M. The assessment of protection treatments on highly porous stones with relation to the sustainability of the interventions on the historical built heritage. In *La Conservazione Del Patrimonio Architettonico All’aperto: Superfici, Strutture, Finiture E Eontesti*; Edizioni Arcadia Ricerche: Marghera/Venezia, Italy, 2012; pp. 477–487.
44. Karapanagiotis, I.; Hosseini, M. Superhydrophobic Coatings for the Protection of Natural Stone. In *Advanced Materials for the Conservation of Stone*; Hosseini, M., Karapanagiotis, I., Eds.; Springer International Publishing: Cham, Switzerland, 2018; pp. 1–25.
45. Esposito Corcione, C.; Striani, R.; Frigione, M. Novel hydrophobic free-solvent UV-cured hybrid organic–inorganic methacrylic-based coatings for porous stones. *Prog. Org. Coat.* **2014**, *77*, 803–812. [[CrossRef](#)]
46. Pinho, L.; Elhaddad, F.; Facio, D.S.; Mosquera, M.J. A novel TiO<sub>2</sub>-SiO<sub>2</sub> nanocomposite converts a very friable stone into a self-cleaning building material. *Appl. Surf. Sci.* **2013**, *275*, 389–396. [[CrossRef](#)]
47. Carmona-Quiroga, P.M.; Martínez-Ramírez, S.; Viles, H.A. Efficiency and durability of a self-cleaning coating on concrete and stones under both natural and artificial ageing trials. *Appl. Surf. Sci.* **2018**, *433*, 312–320. [[CrossRef](#)]
48. Chatzigrigoriou, A.; Manoudis, P.N.; Karapanagiotis, I. Fabrication of Water Repellent Coatings Using Waterborne Resins for the Protection of the Cultural Heritage. *Macromol. Symp.* **2013**, *331–332*, 158–165. [[CrossRef](#)]
49. Pozo-Antonio, J.S.; Rivas, T.; Jacobs, R.M.J.; Viles, H.A.; Carmona-Quiroga, P.M. Effectiveness of commercial anti-graffiti treatments in two granites of different texture and mineralogy. *Prog. Org. Coat.* **2018**, *116*, 70–82. [[CrossRef](#)]
50. La Russa, M.F.; Barone, G.; Belfiore, C.M.; Mazzoleni, P.; Pezzino, A. Application of protective products to “Noto” calcarenite (south-eastern Sicily): A case study for the conservation of stone materials. *Environ. Earth Sci.* **2011**, *62*, 1263–1272. [[CrossRef](#)]
51. Eyssautier-Chuine, S.; Calandra, I.; Vaillant-Gaveau, N.; Fronteau, G.; Thomachot-Schneider, C.; Hubert, J.; Pleck, J.; Gommeaux, M. A new preventive coating for building stones mixing a water repellent and an eco-friendly biocide. *Prog. Org. Coat.* **2018**, *120*, 132–142. [[CrossRef](#)]
52. Aslanidou, D.; Karapanagiotis, I.; Lampakis, D. Waterborne Superhydrophobic and Superoleophobic Coatings for the Protection of Marble and Sandstone. *Materials* **2018**, *11*, 585. [[CrossRef](#)] [[PubMed](#)]
53. Cappelletti, G.; Fermo, P. Hydrophobic and superhydrophobic coatings for limestone and marble conservation. In *Smart Composite Coatings and Membranes: Transport, Structural, Environmental and Energy Applications*; Elsevier: Amsterdam, The Netherlands, 2015; pp. 421–452.
54. Snethlage, R. Stone conservation. In *Stone in Architecture*; Springer: Heidelberg, Germany, 2014; pp. 415–550.
55. Kronlund, D.; Bergbreiter, A.; Meierjohann, A.; Kronberg, L.; Lindén, M.; Grosso, D.; Smått, J.-H. Hydrophobization of marble pore surfaces using a total immersion treatment method–Product selection and optimization of concentration and treatment time. *Prog. Org. Coat.* **2015**, *85*, 159–167. [[CrossRef](#)]
56. Petronella, F.; Pagliarulo, A.; Truppi, A.; Lettieri, M.; Masieri, M.; Calia, A.; Curri, M.L.; Comparelli, R. TiO<sub>2</sub> Nanocrystal Based Coatings for the Protection of Architectural Stone: The Effect of Solvents in the Spray-Coating Application for a Self-Cleaning Surfaces. *Coatings* **2018**, *8*, 356. [[CrossRef](#)]
57. Dumée, L.; Germain, V.; Sears, K.; Schütz, J.; Finn, N.; Duke, M.; Cerneaux, S.; Cornu, D.; Gray, S. Enhanced durability and hydrophobicity of carbon nanotube bucky paper membranes in membrane distillation. *J. Membr. Sci.* **2011**, *376*, 241–246. [[CrossRef](#)]

58. Manoudis, P.N.; Tsakalof, A.; Karapanagiotis, I.; Zuburtikudis, I.; Panayiotou, C. Fabrication of super-hydrophobic surfaces for enhanced stone protection. *Surf. Coat. Technol.* **2009**, *203*, 1322–1328. [[CrossRef](#)]
59. Su, C.; Li, J.; Geng, H.; Wang, Q.; Chen, Q. Fabrication of an optically transparent super-hydrophobic surface via embedding nano-silica. *Appl. Surf. Sci.* **2006**, *253*, 2633–2636. [[CrossRef](#)]
60. de Ferri, L.; Lottici, P.P.; Lorenzi, A.; Montenero, A.; Salvioli-Mariani, E. Study of silica nanoparticles-polysiloxane hydrophobic treatments for stone-based monument protection. *J. Cult. Herit.* **2011**, *12*, 356–363. [[CrossRef](#)]
61. Colangiuli, D.; Calia, A.; Bianco, N. Novel multifunctional coatings with photocatalytic and hydrophobic properties for the preservation of the stone building heritage. *Constr. Build. Mater.* **2015**, *93*, 189–196. [[CrossRef](#)]
62. La Russa, M.F.; Rovella, N.; Alvarez de Buergo, M.; Belfiore, C.M.; Pezzino, A.; Crisci, G.M.; Ruffolo, S.A. Nano-TiO<sub>2</sub> coatings for cultural heritage protection: The role of the binder on hydrophobic and self-cleaning efficacy. *Prog. Org. Coat.* **2016**, *91*, 1–8. [[CrossRef](#)]
63. Milionis, A.; Bayer, I.S.; Loth, E. Recent advances in oil-repellent surfaces. *Int. Mater. Rev.* **2016**, *61*, 101–126. [[CrossRef](#)]
64. Sahasrabudhe, S.N.; Rodriguez-Martinez, V.; O'Meara, M.; Farkas, B.E. Density, viscosity, and surface tension of five vegetable oils at elevated temperatures: Measurement and modeling. *Int. J. Food Prop.* **2017**, *20*, 1965–1981. [[CrossRef](#)]
65. Cansoy, C.E.; Cengiz, U. The effect of perfluoroalkyl and hydrocarbon liquid chain lengths on oleophobic behaviors of copolymer surfaces. *Colloids Surf. A Physicochem. Eng. Asp.* **2014**, *441*, 695–700. [[CrossRef](#)]



© 2018 by the authors. Licensee MDPI, Basel, Switzerland. This article is an open access article distributed under the terms and conditions of the Creative Commons Attribution (CC BY) license (<http://creativecommons.org/licenses/by/4.0/>).